J. exp. Biol. ***195****, 307–328 (1994)*
Printed in Great Britain © The Company of Biologists Limited 1994

AN ELECTROPHYSIOLOGICAL SURVEY OF FROG OLFACTORY CILIA

STEVEN J. KLEENE[1], ROBERT C. GESTELAND[1] AND SHIRLEY H. BRYANT[2]

[1]*Department of Cell Biology, Neurobiology and Anatomy* and [2]*Department of Pharmacology and Cell Biophysics, University of Cincinnati, Cincinnati, OH 45267-0521, USA*

Accepted 15 June 1994

Summary

Individual olfactory receptor neurons vary widely in their responses to odorants. Olfactory stimulus reception occurs in the cilia of the receptor neurons. Thus, the variability among individual neurons could in part be due to differences among the olfactory cilia. We have quantified the known conductance properties of each of 117 frog olfactory cilia. From a strictly qualitative viewpoint, the cilia were very homogeneous. All but a few of them had a basal conductance in the absence of odorants and second messengers, conductances stimulated by cytoplasmic cyclic AMP and by Ca^{2+} and a conductance measured in the presence of ATP and stimulated by GTPγS. However, the magnitudes of the conductances varied widely among the cilia. Amplitudes of the cyclic-AMP- and Ca^{2+}-activated ciliary currents correlated strongly with one another across the 117 cilia and 24 frogs studied, suggesting that expression of the underlying channels may be co-regulated. None of the conductance properties correlated strongly with ciliary length, a marker of cell maturity. Given cytoplasmic MgATP as substrate, ciliary adenylate cyclase apparently produced cyclic AMP, which in turn gated membrane channels and increased the ciliary conductance. In some cilia, MgATP alone caused a very large increase in conductance. In others, there was little effect unless GTPγS, which increases cyclase activity, was also added. No effect of cytoplasmic inositol trisphosphate on ciliary conductance was detectable.

Introduction

Individual olfactory receptor neurons vary widely in their electrical properties (reviewed in Getchell, 1986). In intact olfactory epithelium, some neurons spontaneously generate action potentials at a high rate, while others are silent. Some neurons fail to respond to any odorous stimuli tested, while others are broadly responsive. In patch-clamp studies of isolated olfactory receptor neurons, often a majority of the cells fail to respond to any odorants tested. There is considerable evidence that olfactory stimulus reception and transduction occur in the cilia of the receptor neurons (Kurahashi, 1989;

Key words: olfaction, transduction, receptor neuron, cilia, cyclic-nucleotide-gated channel, calcium-activated chloride channel, cable properties.

Firestein *et al.* 1990; Lowe and Gold, 1991; Dionne, 1992). Thus, the variable electrical properties found among individual neurons may, in part, be due to heterogeneity in the population of olfactory cilia. However, it is not known how one cilium differs from the next.

A wealth of information exists on the average properties of olfactory cilia. Suspensions containing olfactory cilia have an adenylate cyclase, the activity of which is increased by some odorants and by nucleotides that activate G-proteins (Pace *et al.* 1985; Sklar *et al.* 1986; Shirley *et al.* 1986; Bruch and Teeter, 1990; Boekhoff *et al.* 1990). The product of adenylate cyclase activity, cyclic AMP, directly gates channels in the ciliary membrane (Nakamura and Gold, 1987; Kurahashi and Kaneko, 1993), and inward current through these channels mediates the odorant response in intact cells (Kurahashi, 1990; Firestein *et al.* 1991; Lowe and Gold, 1993*a*). Cytoplasmic Ca^{2+} increases the ciliary membrane conductance to Cl^- (Kleene and Gesteland, 1991*b*), and this pathway accounts for some of the olfactory receptor current (Kurahashi and Yau, 1993; Kleene, 1993*b*; Lowe and Gold, 1993*b*). Some odorants increase the activity of phospholipase C in suspensions containing olfactory cilia (Huque and Bruch, 1986; Boekhoff *et al.* 1990; Restrepo *et al.* 1993). One of the products of phospholipase C activity, inositol trisphosphate (InsP_3), gates channels in cultured lobster olfactory neurons (Fadool and Ache, 1992) and in artificial bilayers that include olfactory cilia (Restrepo *et al.* 1990, 1992), and injection of 1,4,5-InsP_3 into olfactory receptor neurons can cause a transient depolarization (Restrepo *et al.* 1990; Miyamoto *et al.* 1992; Okada *et al.* 1994).

It has become routinely possible to measure the electrical properties of individual frog olfactory cilia (Kleene and Gesteland, 1991*a*). We have now quantified these properties in each of 117 cilia. Almost all of the cilia had a basal conductance in the absence of odorants and second messengers, conductances stimulated by cytoplasmic cyclic AMP and Ca^{2+} and a conductance measured in the presence of ATP and stimulated by GTPγS. The magnitudes of these conductances varied widely among the cilia. No effect of cytoplasmic InsP_3 on ciliary conductance was detectable.

Materials and methods

Ciliary patch procedure

Northern grass frogs (*Rana pipiens*) were quickly decapitated and pithed without anesthesia. Single olfactory receptor neurons were isolated from the dorsal or ventral olfactory epithelium by mechanical means without addition of enzymes (Kleene and Gesteland, 1991*a*). The ciliary patch procedure was carried out under phase-contrast microscopy at 600× magnification using a Nikon Diaphot inverted microscope. A neuron or small cluster of cells was transferred to the recording chamber. A recording micropipette (tip diameter about 0.5 μm, resistance 8–10 MΩ) was brought close to one of the cilia and suction was applied until the end of the cilium entered the pipette. Suction was continued until the olfactory vesicle touched the tip of the pipette and a high-resistance seal formed. The patch procedure was videotaped and ciliary lengths were estimated by playing back the video images one frame at a time. For the longer cilia, it

was usually possible with gentle suction to slide the pipette tip along the length of the cilium. When the pipette tip reached the end of the cilium, the cilium was nearly straight, allowing a reliable length measurement.

After sealing the pipette to the base of the cilium, the pipette was raised briefly into the air to excise the cilium from the cell. The cilium remained sealed inside the recording micropipette with the cytoplasmic face of the membrane exposed to the bath. The pipette containing the cilium could be quickly transferred through the air to various pseudointracellular baths without rupturing the seal. Additional details of the ciliary patch procedure have been presented elsewhere (Kleene and Gesteland, 1991*a*).

Solutions

Extracellular solution contained: NaCl, 115 mmol l^{-1}; KCl, 3 mmol l^{-1}; Hepes, 5 mmol l^{-1}; $MgCl_2$, 2 mmol l^{-1}; $CaCl_2$, 1 mmol l^{-1}; and NaOH, 2 mmol l^{-1} (pH 7.2). Extracellular solution was used to bathe intact cells and to fill the recording pipettes. Patch formation was also accomplished in extracellular solution. After a cilium had been excised from a neuron, the pipette containing the cilium was transferred through a series of six pseudointracellular solutions which bathed the cytoplasmic face of the ciliary membrane. The six pseudointracellular solutions used are defined in Table 1. All were adjusted to pH 7.2. $[Ca^{2+}]_{free}$ was buffered with Bapta [1,2-bis(*o*-aminophenoxy)ethane-*N*,*N*,*N*′,*N*′-tetraacetic acid], a highly Ca^{2+}-specific chelator (Tsien, 1980). $[Ca^{2+}]_{free}$ was calculated using apparent association constants K'_{Ca} determined in triplicate by the method of Bers (1982). The K'_{Ca} values were 6.62×10^6 l mol^{-1} in 115 mmol l^{-1} KCl and 7.76×10^6 l mol^{-1} in 115 mmol l^{-1} *N*-methyl-D-glucamine (NMDG) chloride, both containing 5 mmol l^{-1} Hepes and adjusted to pH 7.2. In all but the high-Ca^{2+} pseudointracellular solution, $[Ca^{2+}]_{free}$ was 0.15 μmol l^{-1}. Bapta was included in the high-Ca^{2+} solution for consistency, even though its buffering capacity was exceeded.

Table 1. *Compositions of pseudointracellular solutions (mmol l^{-1})*

	Control	Na^+-, K^+-free	ATP	High-Ca^{2+}	Cyclic AMP	ATP+ GTPγS
NaCl	5	–	5	5	5	5
KCl	110	–	110	110	110	110
NMDG-Cl	–	115	–	–	–	–
KOH	9	–	17	9	9	17
Tris base	–	9	–	–	–	–
Hepes	5	5	5	5	5	5
Bapta	2	2	2	2	2	2
$CaCl_2$	1	1	1	2.3	1	1
$MgCl_2$	2	2	2	2	–	2
ATP	–	–	2	–	–	2
Li_4GTPγS	–	–	–	–	–	0.1
Cyclic AMP	–	–	–	–	0.1	–
IBMX	–	–	0.1	–	–	0.1

IBMX, 3-isobutyl-1-methylxanthine; NMDG-Cl, *N*-methyl-D-glucamine chloride.

Solutions were designed so that the ligand-activated conductances reversed close to 0 mV. Ionic concentrations in the cilium *in vivo* are unknown.

The solutions labeled 'ATP', 'cyclic AMP' and 'ATP+GTPγS' [GTPγS, guanosine 5′-*O*-(3-thiotriphosphate)] were designed for studying the cyclic-AMP-activated conductance. To avoid reduction of this conductance by cytoplasmic Mg^{2+} (Kleene, 1993*a*), these three solutions contained little free Mg^{2+}. In the cyclic AMP solution, Mg^{2+} was not added. In the ATP and ATP+GTPγS solutions, ATP and Mg^{2+} were both present at 2 mmol l^{-1}. We estimate that $[Mg^{2+}]_{free}$ was 0.3 mmol l^{-1} in these two solutions, and the cyclic-AMP-activated current at positive potentials showed little evidence of open-channel block (see Fig. 2, trace B). Although reduction of cytoplasmic Mg^{2+} concentration prevented inhibition of the cyclic-AMP-activated current at positive potentials, the current at negative potentials was greatly reduced by the presence of divalent cations in the pipette solution (Nakamura and Gold, 1987; Dhallan *et al.* 1990; Zufall and Firestein, 1993).

A low level of cyclic AMP phosphodiesterase activity was detectable in the cilia (not shown). This activity reduced the small currents measured in the presence of ATP, so the phosphodiesterase inhibitor IBMX (3-isobutyl-1-methylxanthine) was added to the ATP and ATP+GTPγS solutions. IBMX was added from a stock solution in dimethylsulfoxide. The final concentration of dimethylsulfoxide was 0.1 % (w/v), which alone did not affect the ciliary conductance. Ciliary phosphodiesterase activity had no effect in the presence of saturating levels of cyclic AMP, so IBMX was not added to the cyclic AMP solution.

Pseudointracellular solutions were tested in the order shown in Table 1 (control first). In general, the order was unimportant, and it was possible to return to any solution and repeat a previous measurement. There was one exception to this: the effect of GTPγS was irreversible. A cilium exposed to GTPγS continued to show the maximal ATP-dependent current even after removal of the GTPγS. On return to the control bath, which lacked ATP, it was possible to verify the original control measurement. This was often done to ensure that the seal resistance had not decreased during the experiment. In all but one of the baths, the current–voltage (*I–V*) relationship became stable within 10 s after placing the pipette in the bath. However, activation by GTPγS (the ATP+GTPγS bath) took as long as 4 min. Current–voltage relationships were not recorded until they had become stable.

Electrical recording

Both the recording pipette and chamber were coupled to a List L/M-EPC7 patch-clamp amplifier by Ag/AgCl electrodes, each bathed in extracellular solution. All recordings were carried out under voltage-clamp at room temperature (25 °C). Current was adjusted to zero with the open pipette in the well in which the patching procedure was carried out. Both the bath and the tip of the pipette contained extracellular solution at this stage. After excision of a cilium, the pipette was transferred through a series of six wells containing the pseudointracellular solutions. Each of these wells was connected by a salt bridge to a common reference bath. The salt bridge contained extracellular solution plus 5 % (w/v) agarose (Sigma Type I). A correction was applied for the liquid junction potential

between each pseudointracellular bath and its salt bridge (Hagiwara and Ohmori, 1982). The measured potentials of the pseudointracellular solutions relative to the salt bridge were: control, −2.7 mV; Na^+-, K^+-free, +4.9 mV; ATP, −3.2 mV; high-Ca^{2+}, −2.7 mV; cyclic AMP, −3.2 mV; ATP+GTPγS, −3.2 mV.

Voltage ramps (+100 to −100 mV membrane potential, 0.2 mV ms^{-1}) were generated by pCLAMP software (Axon Instruments). Current–voltage records were acquired at a sampling rate of 500 Hz. In most cases, three replicate ramps were averaged to reduce noise. Currents measured during voltage jumps were nearly equal to currents at the same voltages on the ramps. In all records, an upward deflection represents increasing positive current from the bath into the pipette. Potentials are reported as bath (cytoplasmic) potential relative to pipette potential. To estimate a reversal potential, a 10 mV region surrounding the apparent reversal potential was fitted to a straight line. The voltage intercept of this line was taken as the reversal potential. Current values at a given voltage were calculated by averaging a 10 mV region surrounding the given voltage. Results of repeated experiments are reported as mean ± S.E.M. The Student's *t*-test was used for statistical comparisons. Significance levels are reported for two tails.

Correction of current–voltage relationships

The *I–V* plot in the control bath (see Fig. 2, trace A) was subtracted from one acquired in one of the baths designed to activate ligand-gated channels (see Fig. 2, traces B–E). The resulting difference *I–V* plot showed conductance due to the cytoplasmic effectors in the bath (ATP, Ca^{2+}, etc.). Slope conductances were taken from the difference *I–V* plots and measured at potentials where the ligand-activated current was large relative to control. Conductance activated by cyclic AMP was measured between +60 and +90 mV. There was no contamination by the secondary Cl^- current at this potential (Kleene, 1993*b*). Conductance activated by Ca^{2+} was measured between −50 and 0 mV. In all cases, specific conductances are reported. The measured input slope conductances were corrected for the ciliary cable properties and normalized to membrane surface area as described in the Appendix.

Basal ciliary conductance was determined as described elsewhere (Kleene, 1992). The *I–V* relationship was recorded first with the cilium in the control pseudointracellular bath and then in the Na^+-, K^+-free bath. The *I–V* relationship in the second bath was corrected for free solution conductances and subtracted from the *I–V* relationship in the first bath. The remaining basal conductance was attributed to the ciliary membrane (Kleene, 1992). Na^+ and K^+ were not replaced in the pipette in this study, so the basal conductance at negative potentials would have been underestimated (Kleene, 1992) and is not discussed.

Materials

DCB (3′,4′-dichlorobenzamil, an amiloride derivative) was generously provided by Dr Gregory Kaczorowski (Merck, Rahway, New Jersey). DCB blocks the ciliary cyclic-AMP-activated current but not the Ca^{2+}-activated Cl^- current (Kleene, 1993*b*). DCB also blocks certain other channels and exchangers (Garcia *et al.* 1990). 1,4,5-InsP_3 (D-*myo*-inositol 1,4,5-trisphosphate, trilithium salt) was purchased from Calbiochem, and all other reagents were from Sigma.

Results

Ciliary characteristics

To determine the heterogeneity of frog olfactory cilia, several characteristics of each of 117 single cilia were measured. Cilia were obtained from 24 different animals and from both the dorsal (N=57) and ventral (N=60) olfactory epithelia. No two cilia were from the same neuron. Electrical properties of each cilium were determined by the ciliary patch method (Kleene and Gesteland, 1991*a*). One cilium of a cell was sucked inside a patch pipette. A high-resistance seal was made between the base of a cilium and the tip of the pipette, and the pipette containing the cilium was detached from the cell. The cilium remained inside the pipette with the cytoplasmic face of its membrane exposed to the bath (Kleene and Gesteland, 1991*a*). Neurons were easily distinguished from respiratory epithelial cells. Each respiratory cell bore several dozen cilia up to 12 μm long. These beat synchronously, while the neuronal cilia (12–127 μm) moved independently of one another. In 44 % of the neurons used in this study, action potentials were detectable through the ciliary membrane during the patch procedure (Kleene and Gesteland, 1991*a*).

The length of each cilium was measured, together with the following electrical properties of the ciliary membrane: the basal conductance in the absence of odorants and second messengers (Kleene, 1992); conductances activated by cytoplasmic cyclic AMP (Nakamura and Gold, 1987; Kurahashi and Kaneko, 1993) and Ca^{2+} (Kleene and Gesteland, 1991*b*); and a conductance observed in the presence of cytoplasmic ATP and GTPγS. These ciliary characteristics are discussed in detail in the following sections.

Ciliary lengths

In this study, we measured the length of each cilium as a marker of the developmental age of its receptor neuron. Olfactory receptor neurons are continually replaced during the life of the animal. As an individual neuron matures, its cilia lengthen. If the epithelium is deciliated, new cilia grow rapidly (about 20 μm per day) until they reach the length that is appropriate to the developmental age of the cell (Mair *et al.* 1982; Adamek *et al.* 1984). Stages in cell development can also be assessed by the ciliary mechanical properties. Newly differentiated receptor neurons have short cilia which move rapidly and asynchronously. After a few days of maturation, the cilia move more slowly and metachronally and have lengths between about 10 and 30 μm. After 2–3 weeks of development, the cilia become immotile and grow in length beyond 30 μm at a slow rate. Some cells have cilia as long as 250 μm. The length distribution of the excised cilia used in this study is shown in Fig. 1. The distribution is similar to that measured in intact epithelia (P. A. Farmer and R. C. Gesteland, unpublished observations). For unknown reasons, it was very difficult to obtain high-resistance seals with the longest cilia.

The length of each cilium studied was measured from videotapes made during the ciliary patch procedure. By repeatedly sucking the tip of a cilium into a patch pipette and then releasing it, it was possible in four cases to estimate the reproducibility of the ciliary length measurements. For these cilia, the lengths were found to be: 57±4 μm (N=7, range 52–60 μm); 31±3 μm (N=8, range 27–37 μm); 39±3 μm (N=12, range 35–43 μm); and

45±6 μm (N=13, range 32–52 μm). In only one of these cases did a single value deviate from the mean by more than 20 %.

There was no evidence that the cilia studied had broken during cell isolation. In most cases, the several cilia of a given cell appeared to be of one length, an unlikely consequence of random breakage. Cilia on the isolated cells showed motility consistent with observations of intact epithelia (Mair *et al.* 1982). The shortest cilia moved very rapidly. Those of intermediate length moved in a slow, whip-like fashion, and only the longest cilia were immotile. On rare occasions, stretching a cilium or sucking it into a pipette that was too small damaged the ciliary membrane. In this case, obvious blebs of membrane formed and the cilium was rejected.

Basal conductance

In the absence of odorants and second messengers, the ciliary membrane has a small basal conductance to cations, primarily to Na^+ and K^+ (Kleene, 1992) but also to Ca^{2+} (Kleene, 1993*b*). More current passes through this conductance at positive than at negative potentials (Kleene, 1992). All but 17 of the cilia in this study showed a basal conductance between +60 and +90 mV. The measured input conductance was corrected for the ciliary cable properties and normalized to membrane surface area. For all of the cilia, the basal specific conductance averaged 9±1 pS μm^{-2} (N=117, range 0–62 pS μm^{-2}). The space constant λ for electrotonic conduction averaged 154±15 μm (N=100), in accordance with a previous estimate (Kleene, 1992). In the absence of odorants and second messengers, the ciliary length was shorter than λ by a factor that averaged 0.37±0.05 (N=100).

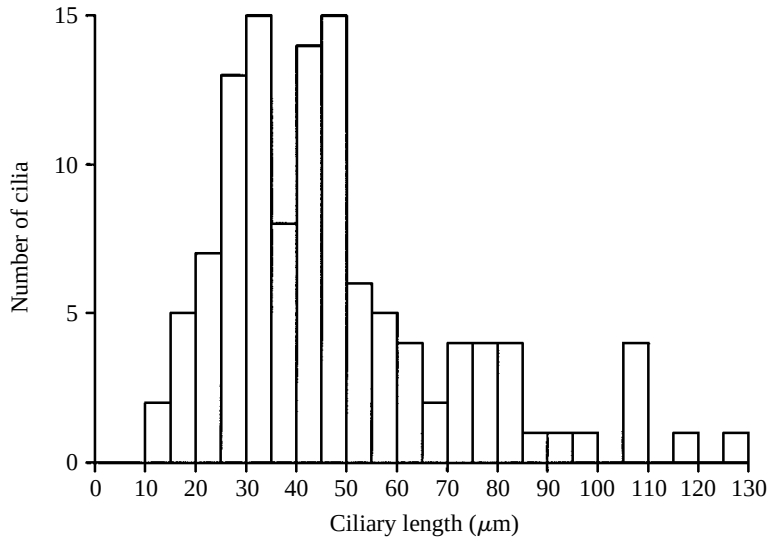

Fig. 1. Distribution of ciliary lengths. Lengths were measured by playing back a videotape of the ciliary patch procedure one frame at a time. Lengths are shown for all 117 cilia used in this study. The mean ciliary length was 47±2 μm (N=117, range 12–127 μm); cilia were selected to include the whole spectrum of available lengths.

Cyclic-AMP-activated conductance

Addition of cyclic AMP to the cytoplasmic face of the ciliary membrane increases the membrane conductance to cations (Nakamura and Gold, 1987; Kurahashi and Kaneko, 1993; Kleene and Gesteland, 1991*a*). The conductance barely discriminates between Na^+ and K^+ (Nakamura and Gold, 1987; Kurahashi, 1990; Dhallan *et al*. 1990; Frings *et al.* 1992), so the reversal potential in normal solutions is in the region of 0 mV. Inward current through the cyclic-AMP-activated conductance is blocked by divalent cations in the extracellular medium (Nakamura and Gold, 1987; Dhallan *et al.* 1990; Zufall and Firestein, 1993). In the frog, outward current is blocked by cytoplasmic Mg^{2+} (Kleene, 1993*a*). For this study, we retained extracellular Ca^{2+} and Mg^{2+} but eliminated cytoplasmic Mg^{2+}. Thus, the cyclic-AMP-activated current was strongly blocked only at negative potentials (Fig. 2, trace B). A concentration of cyclic AMP (100 μmol l^{-1}) that elicited maximal responses was used.

Every cilium examined showed some cyclic-AMP-activated conductance (Fig. 3A). Between +60 and +90 mV, the specific conductance averaged 2.5±0.2 nS μm^{-2} (*N*=117, range 0.005–11.3 nS μm^{-2}). The reversal potential of the cyclic-AMP-activated current averaged –0.2±0.3 mV (*N*=108, range −17.2 to +8.4 mV; nine cilia with currents of less than 100 pA at +80 mV were not included). In three of the four cilia with the smallest

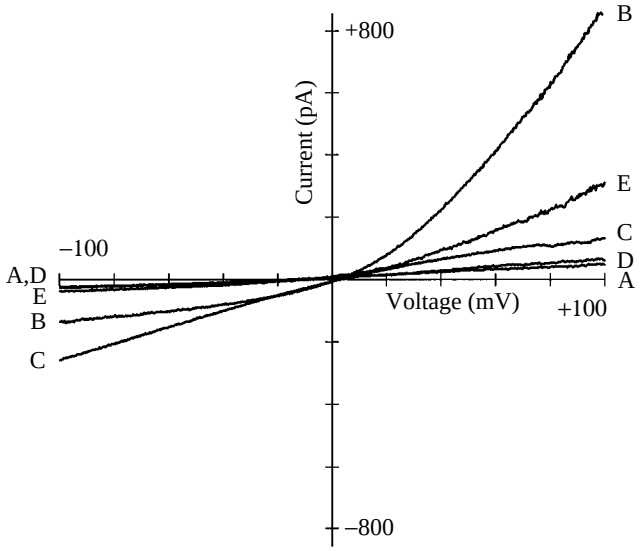

Fig. 2. *I–V* relationships for the ligand-activated conductances studied. The records are all from one 40 μm long cilium. Each trace is the average of three successive determinations. The recording pipette contained extracellular solution, and the bath one of the pseudointracellular solutions as follows: (A) control; (B) cyclic AMP (control+100 μmol l^{-1} cyclic AMP); (C) high-Ca^{2+} (control+300 μmol l^{-1} free Ca^{2+}); (D) ATP (control+2 mmol l^{-1} ATP); and (E) ATP+GTPγS (control+2 mmol l^{-1} ATP+100 μmol l^{-1} GTPγS). The only correction applied to the *I–V* curves as shown was for the liquid junction potential at the salt bridge. The control (A) has not been subtracted from any of the curves.

cyclic-AMP-activated currents (10–50 pA at +80 mV), it was possible to show repeatedly that current increased when the cilium was transferred from the cyclic-AMP-free control bath to the cyclic-AMP-containing bath. Even these smallest cyclic-AMP-activated conductance increases showed the outward rectification characteristic of cyclic AMP activation. Between +60 and +90 mV, the ciliary space constant λ in the presence of 100 μmol l^{-1} cyclic AMP averaged 14±2 μm (N=117, range 3–130 μm). Under these

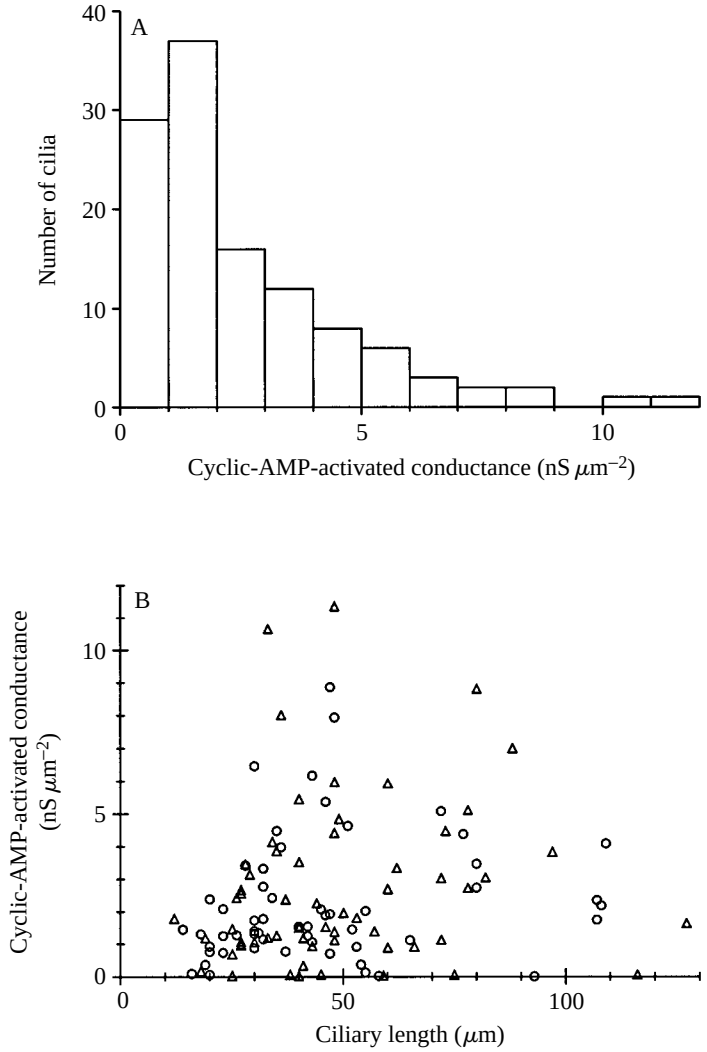

Fig. 3. Ciliary cyclic-AMP-activated conductance. (A) Distribution of cyclic-AMP-activated specific conductance in 117 cilia. Slope conductance was measured between +60 and +90 mV, corrected for ciliary cable properties, and normalized to membrane area as described in the Appendix. (B) Cyclic-AMP-activated specific conductance as a function of ciliary length for 117 cilia. The correlation coefficient is +0.15, which is not significant (P>0.10). ○, cilia from neurons of the dorsal epithelium; △, cilia from neurons of the ventral epithelium.

conditions, the ciliary length was on average 6.8±0.5 (N=117, range 0.2–24) times the space constant. There was no significant correlation between the length of a cilium and the cyclic-AMP-activated specific conductance (Fig. 3B).

The magnitude of the cyclic-AMP-activated increase in specific conductance can be used to estimate the average density of the cyclic-AMP-gated channels in the proximal ciliary membrane. Single-channel conductance is assumed to be 15 pS [measured in the frog by Frings *et al.* (1992)] and the maximum open probability 0.80 (Kurahashi and Kaneko, 1993). Dividing the cyclic-AMP-activated specific conductance by the single-channel conductance and the maximum open probability gave a channel density averaging 205±18 channels μm^{-2} (N=117, range 0.5–944 channels μm^{-2}).

Ca^{2+}-activated conductance

The conductance of the ciliary membrane increases when cytoplasmic free Ca^{2+} concentration exceeds 2 $\mu mol\,l^{-1}$ (Kleene and Gesteland, 1991*b*). Cl^- carries the Ca^{2+}-activated current, so the reversal potential in normal solutions is close to 0 mV (Kleene and Gesteland, 1991*b*). At the saturating levels of free Ca^{2+} used here (300 $\mu mol\,l^{-1}$), the conductance shows some inward rectification (Fig. 2, trace C). All but four of the cilia in this study showed a Ca^{2+}-activated conductance (Fig. 4A). For all cilia, the specific Ca^{2+}-activated conductance averaged 0.22±0.03 nS μm^{-2} (N=117, range 0–2.5 nS μm^{-2}). The reversal potential of the Ca^{2+}-activated current averaged –0.1±0.3 mV (N=109, range −9.4 to +9.2 mV; eight cilia with currents more positive than −25 pA at −80 mV were not included). The inward rectification characteristic of activation by saturating levels of Ca^{2+} was evident even when the current was small. The ciliary space constant λ in the presence of 300 $\mu mol\,l^{-1}$ Ca^{2+} averaged 35±3 μm (N=113, range 6–287 μm). Under these conditions, the ciliary length was on average 2.0±0.2 (N=113, range 0.1–12) times the space constant.

There was no significant correlation between the length of a cilium and the Ca^{2+}-activated specific conductance (Fig. 4B). However, a strong correlation was found between the amplitudes of the two ligand-activated conductances across the population of cilia (Fig. 5). Cilia that had a large cyclic-AMP-activated conductance also showed a large Ca^{2+}-activated conductance; in other cilia, the levels of both currents were low. The 117 cilia in this study came from 24 frogs, but anywhere from one to ten cilia were used from each frog. Thus, the correlation shown in Fig. 5 has been strongly influenced by a few individual frogs. It is possible to weight each animal equally by including just one point per frog, that point being the mean of all current measurements in that frog. In such a plot (not shown), the correlation between cyclic-AMP- and Ca^{2+}-activated conductances still holds across the population of 24 frogs studied (r=0.68, P<0.0005).

ATP-dependent conductance

When 2 $mmol\,l^{-1}$ MgATP was added to the cytoplasmic bath, the ciliary membrane conductance increased (Fig. 2, trace D). When both 2 $mmol\,l^{-1}$ ATP and 100 $\mu mol\,l^{-1}$ GTPγS were included in the bath, the conductance increased further (Fig. 2, trace E). It is likely that the ciliary adenylate cyclase (Pace *et al.* 1985; Sklar *et al.* 1986; Shirley *et al.* 1986; Bruch and Teeter, 1990; Boekhoff *et al.* 1990) converted some of the ATP to cyclic

AMP, which in turn opened cyclic-AMP-gated channels. Three lines of evidence are consistent with this mechanism. First, the activated current showed the strong outward rectification and reversal potential close to 0 mV (Fig. 2, traces D,E) that are characteristic of the cyclic-AMP-activated conductance under the ionic conditions used here. Second, the current was increased by GTPγS (Fig. 2, trace E) and also by 10–100 μmol l^{-1} forskolin (not shown), both of which stimulate the olfactory adenylate

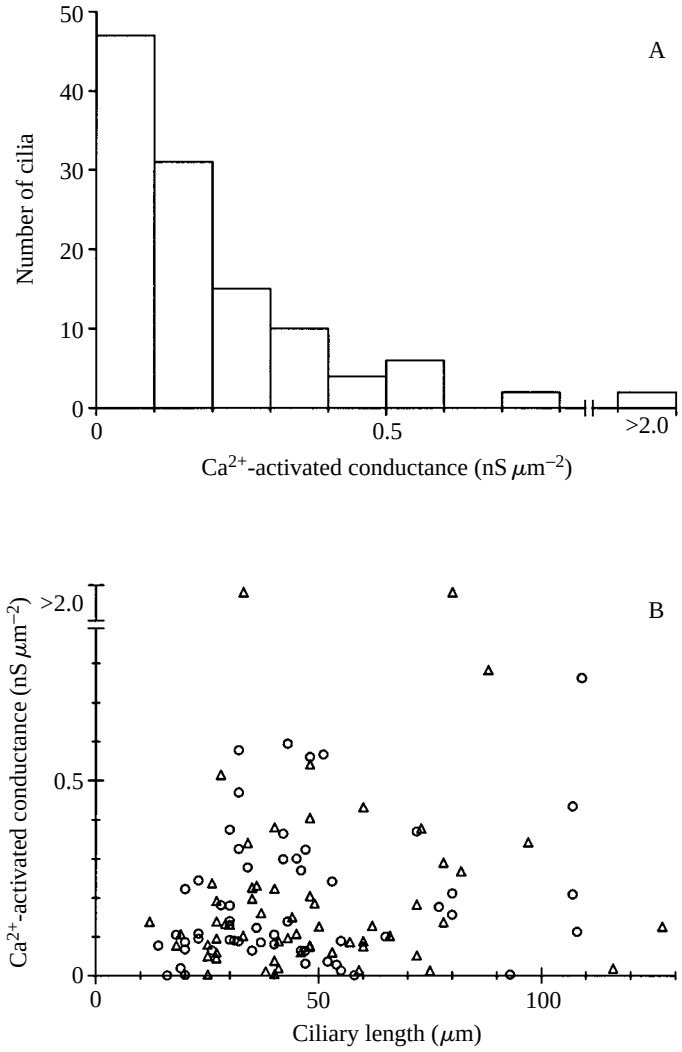

Fig. 4. Ciliary Ca^{2+}-activated conductance. (A) Distribution of Ca^{2+}-activated specific conductance in 117 cilia. Slope conductance was measured between −50 and 0 mV, corrected for ciliary cable properties, and normalized to membrane area as described in the Appendix. The two cilia in the bin at the far right had specific conductances of 2.1 and 2.5 nS μm^{-2}. (B) Ca^{2+}-activated specific conductance as a function of ciliary length for 117 cilia. The correlation coefficient is +0.14, which is not significant (P>0.10). ○, cilia from neurons of the dorsal epithelium; △, cilia from neurons of the ventral epithelium.

cyclase (Pace *et al.* 1985; Sklar *et al.* 1986; Shirley *et al.* 1986; Bruch and Teeter, 1990; Boekhoff *et al.* 1990). Third, the current due to ATP and GTPγS was blocked by 100 μmol l^{-1} cytoplasmic DCB, which blocks the olfactory cyclic-AMP-activated current (Kolesnikov *et al.* 1990; Kleene, 1993*b*). Inhibition averaged 85±4 % at +80 mV (*N*=6, range 69–97 %).

The specific conductance activated by ATP and GTPγS was measured in each of the 117 cilia. Fig. 6A shows the unstimulated and GTPγS-stimulated levels of this conductance in each cilium. All but seven cilia showed some conductance due to addition of 2 mmol l^{-1} ATP to the cytoplasmic bath. For all of the cilia, this conductance averaged 75±16 pS μm^{-2} (*N*=117, range 0–1600 pS μm^{-2}). At −50 mV, the resting potential of the neuron (Pun and Gesteland, 1991), little inward current resulted from the presence of ATP (mean −13±4 pA, range −374 to +14 pA, *N*=117). ATP alone caused very large conductance increases in a few cilia (Fig. 6A); elimination of six of these from the average reduced the mean current at −50 mV to −6 pA.

In all but six of the cilia, the presence of both 2 mmol l^{-1} ATP and 100 μmol l^{-1} GTPγS in the cytoplasmic bath resulted in greater conductance than when ATP was added alone (Fig. 6A). This is apparently due to stimulation of the ciliary adenylate cyclase by GTPγS. We calculated the ratio of specific conductances in the presence and absence of GTPγS (with ATP present in either case, Fig. 6B). GTPγS increased specific conductance between +60 and +90 mV by a factor that averaged 9.3±1.0 (*N*=106, range

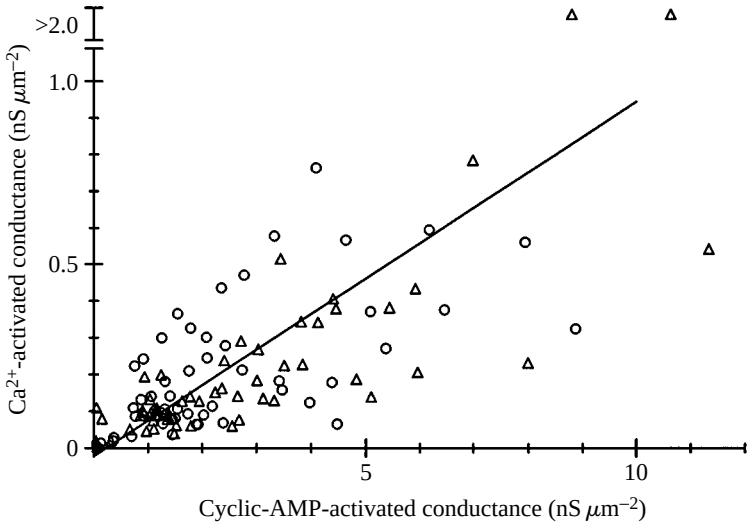

Fig. 5. Correlation between ciliary cyclic-AMP- and Ca^{2+}-activated conductances. Specific conductances were determined as described for Figs 4 and 5. One point is shown for each of 117 cilia, together with the linear least-squares line. The line has a slope of +0.097 and an *x*-intercept of +0.24. The correlation coefficient is +0.68, which is significant (P<0.0001). ○, cilia from neurons of the dorsal epithelium; △, cilia from neurons of the ventral epithelium. The two points plotted in the region marked >2.0 had specific Ca^{2+}-activated conductances of 2.1 and 2.5 nS μm^{-2}. Note that the conductance values shown depend strongly on the voltages used to determine them (Fig. 2, traces B,C).

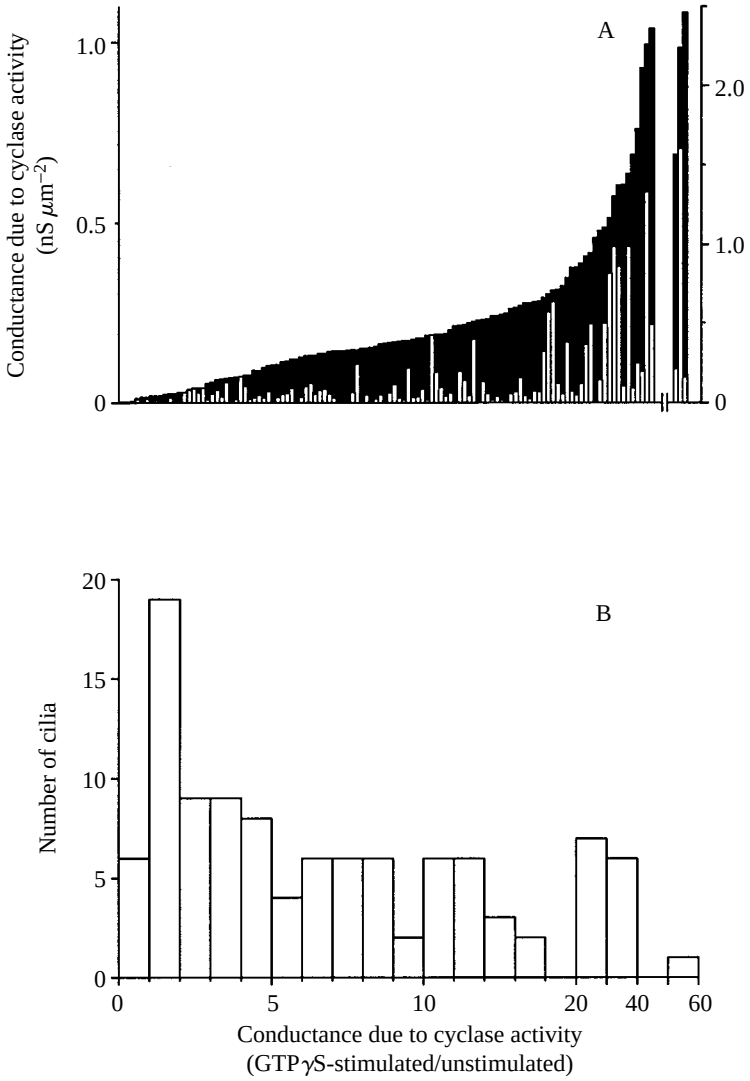

Fig. 6. (A) Specific conductance between +60 and +90 mV due to the addition of cytoplasmic ATP and GTPγS in 117 cilia. The total height of each bar shows conductance measured in the presence of both ATP and GTPγS. The lower (white) part of each bar shows conductance measured in the presence of ATP alone. Cilia are ranked in order of increasing maximal conductance. Six cilia that showed a slight conductance decrease in the presence of GTPγS are shown as entirely white bars. This decrease never exceeded 0.07 nS μm^{-2}. The vertical scale on the right applies to the last three bars only, which are separated from the other 114 bars by a gap. (B) Ratios of specific conductance due to ATP in the presence and absence of GTPγS for 106 cilia. Ratios could not be reliably determined for cilia with conductances below 0.003 nS μm^{-2} in the presence of ATP alone, so conductances from these cilia (N=11) were eliminated from this part of the figure. For each remaining cilium, the total bar height from A (maximal conductance) was divided by the height of the white portion of the bar (conductance in the absence of GTPγS). Note that the bin width for the conductance ratio is 1 for ratios from 1 to 10, 2 for ratios from 10 to 20 and 10 for ratios from 20 to 60.

0.6–58). Two-thirds of the population showed stimulation by a factor within the range 1.1–10.0. In no cilium was the conductance activated by ATP plus GTPγS as high as that measured in the presence of a saturating level of cyclic AMP. It is important to note that the conductance measured here is not directly proportional to adenylate cyclase activity, since the number of channels activated is not directly proportional to cyclic AMP concentration (Nakamura and Gold, 1987; Frings *et al.* 1992). This conductance showed no correlation with ciliary length in the absence or presence of GTPγS (P>0.10 in either case).

1,4,5-inositol trisphosphate

In suspensions containing rat (Boekhoff *et al.* 1990) or catfish (Restrepo *et al.* 1993) olfactory cilia, some odorants cause an increase in InsP_3 production. Injection of 1,4,5-InsP_3 into catfish (Restrepo *et al.* 1990; Miyamoto *et al.* 1992) or rat (Okada *et al.* 1994) olfactory receptor neurons can cause a transient depolarization. In artificial bilayers which included catfish (Restrepo *et al.* 1990) or rat (Restrepo *et al.* 1992) olfactory cilia, it was found that 1,4,5-InsP_3 activated single channels that conducted Ba^{2+}. However, in frog olfactory cilia, we have failed to find any effect of 1,4,5-InsP_3 on ciliary membrane conductance. The *I–V* relationship was identical in the control pseudointracellular bath and in the same bath with 100 μmol l^{-1} InsP_3 added (not shown, N=26). The pipette contained the standard extracellular solution. The presence of the ciliary membrane was verified by demonstrating a conductance increase in the high-Ca^{2+} bath.

Addition of fluoride to the cytoplasmic solution increases the effectiveness of InsP_3 in catfish olfactory neurons (Restrepo *et al.* 1990; Miyamoto *et al.* 1992). Even after replacing 30 mmol l^{-1} KCl in the bath solutions with 30 mmol l^{-1} KF, we still found no effect of 100 μmol l^{-1} cytoplasmic InsP_3 on ciliary conductance (N=15). In other experiments, 75 mmol l^{-1} NaCl in the standard extracellular (pipette) solution was replaced with 50 mmol l^{-1} $BaCl_2$; Ba^{2+} is a good current carrier for the InsP_3-gated channel derived from catfish (Restrepo *et al.* 1990) or rat (Restrepo *et al.* 1992) olfactory cilia. Again, 100 μmol l^{-1} InsP_3 had no effect on the ciliary *I–V* relationship, with (N=7) or without (N=7) the F^- substitution described above.

Clogged patch pipettes

In previous studies of excised single cilia, a minority of the cilia showed little or no response either to cytoplasmic cyclic AMP (Kleene and Gesteland, 1991*a*) or to Ca^{2+} (Kleene and Gesteland, 1991*b*). In those cases, the high resistance at the pipette tip could have been due either to a ciliary membrane with few channels or to some non-specific obstruction of the pipette tip. The present study provided an opportunity to make that distinction. A clogged pipette should show no response to either cyclic AMP or Ca^{2+}. In addition, the leakage conductance measured in the control bath should be entirely accounted for as a non-selective shunt (Kleene, 1992). In other words, the leakage should not be larger in Na^+, K^+-containing solutions than in solutions of $NMDG^+$, after correction for the free solution conductances (Kleene, 1992). In this study, only three pipette tips were judged by these criteria to have been non-specifically obstructed. Results from those experiments were excluded from the rest of the study.

Discussion

We have measured the membrane conductance properties of 117 individual frog olfactory cilia. From a strictly qualitative viewpoint, the population of cilia was almost perfectly homogeneous. The cilia have a basal conductance in the absence of odorants and second messengers, conductances stimulated by cytoplasmic cyclic AMP and Ca^{2+}, and a conductance measured in the presence of ATP and stimulated by GTPγS. None of these properties was missing in more than a few of the 117 cilia. Similarly, a cyclic-AMP-activated current is found in most olfactory receptor neurons that retain their cilia (Kurahashi, 1990; Frings and Lindemann, 1991). However, we found that the magnitudes of the ciliary conductances varied widely. Even after eliminating 5 % of the data at each extreme, the specific conductances activated by cyclic AMP and by Ca^{2+} varied over ranges of 220-fold and 34-fold, respectively. It is possible that the variability is smaller in intact cells, as has been suggested for rod photoreceptors (Karpen *et al.* 1992). Clogged pipettes were not the cause of the lowest conductances, which still showed characteristic rectification. Most conductances stabilized within 10 s, indicating that diffusion of ligand into the cilium was also not a limiting factor. Modulation of the cyclic-AMP-gated channels by Ca^{2+}-calmodulin (Chen and Yau, 1994) was probably not a factor, since we maintained cytoplasmic free Ca^{2+} concentration at 0.15 μmol l^{-1}.

Having measured the specific conductance activated by cyclic AMP in single cilia, we estimated the density of the ciliary cyclic-AMP-gated single channels. On average, the proximal ciliary membrane contained 205 channels μm^{-2}, and the highest estimate for any single cilium was 944 channels μm^{-2}. Higher estimates resulted when patches of membrane were excised from the side of the cilium (Nakamura and Gold, 1988; Kurahashi and Kaneko, 1993). Estimates of 450–7000 channels μm^{-2} resulted from one such study (Nakamura and Gold, 1988). In the other, a mean density of 1750 channels μm^{-2} (varying over a 15-fold range) was found in the toad (Kurahashi and Kaneko, 1993). These high values are probably not due to high local channel concentrations; channel density is reportedly uniform over much of the ciliary length (Lowe and Gold, 1993*a*; Kurahashi and Kaneko, 1993). In both studies, however, the area of the excised patch was assumed to equal the cross-sectional area of the pipette tip (Nakamura and Gold, 1988; Kurahashi and Kaneko, 1993). This is undoubtedly an underestimate of the true patch area, resulting in an overestimate of channel density (Karpen *et al.* 1992). Our own estimate may be a little low; even at positive potentials, external divalent cations cause a small reduction of cyclic-AMP-activated current. Our estimate of channel density also depends on a model of the ciliary cable conduction properties, as described in the Appendix. The density of channels underlying the Ca^{2+}-activated current cannot be estimated, since the single-channel conductance is unknown.

The amplitudes of the cyclic-AMP- and Ca^{2+}-activated currents correlated strongly across the population of 117 cilia and across the population of 24 frogs. Thus, expression of the underlying channels may be co-regulated. In amphibians (Kurahashi and Yau, 1993) and rat (Lowe and Gold, 1993*b*), the olfactory receptor current is a mixture of these

two currents. Ca^{2+} entering through the cyclic-AMP-gated channels activates the secondary Cl^- current (Kleene, 1993*b*). It would make sense to maintain a balance between the levels of these two conductances, as we found. As mucosal [Ca^{2+}] increases, the cyclic-AMP-gated channels are blocked (Zufall and Firestein, 1993), but the secondary Cl^- current increases (Kleene, 1993*b*). Thus, the receptor current could remain fairly constant even though the mucosal environment may vary (Kurahashi and Yau, 1993). In olfactory neurons having a negative equilibrium potential for Cl^- (Dubin and Dionne, 1994), a Ca^{2+}-activated Cl^- current could help to limit or terminate the initial depolarization.

Among vertebrates, there is evidence from catfish and rat that InsP_3 may play some role in odorant transduction. We were unable to detect any effect of InsP_3 on the conductance of frog olfactory cilia. Other workers have injected InsP_3 into amphibian olfactory receptor neurons and also found no effect (Firestein *et al.* 1991; Lowe and Gold, 1993*a*). However, membrane patches from the soma or dendrite of bullfrog receptor neurons are a source of InsP_3-gated channels (Suzuki, 1993). Our results indicate that these channels may not be present in the cilia of frogs.

In frog olfactory epithelium, response properties vary with the developmental age of the neurons. There are clear differences in responsiveness to odors as olfactory epithelium regenerates after ablation of the receptor neurons. In the early stages of regeneration, cells are not very responsive to odors, and amplitudes of the receptor current (electro-olfactogram or EOG) increase linearly with time for 3–4 weeks. Responsiveness to individual odors increases in amplitude at rates characteristic of the odor. At about 4 weeks of regrowth, when the cilia become immotile, EOG amplitudes increase abruptly, achieving the amplitudes encountered in the mature epithelium of an adult frog (Adamek *et al.* 1984; Lidow *et al.* 1987). In the present study, ciliary length was used as a marker of the developmental age of the neuron. None of the ciliary conductances correlated strongly with ciliary length. Apparently the membrane conductance processes that support transduction are present in cilia at all developmental stages. Other evidence suggests that ontogeny of signal-transduction proteins roughly coincides with ciliogenesis (Menco *et al.* 1994). The differences in the EOG measured during development and regeneration may instead reflect changes in the population of odor receptors, which we have not studied. There were no significant differences for any of the ligand-activated conductances measured when cilia from neurons of the dorsal epithelium were compared with those of ventral origin.

The most interesting variability among the cilia was in the conductance activated by ATP and GTPγS. It is likely that this conductance reflects adenylate cyclase activity. Given cytoplasmic MgATP as substrate, the ciliary cyclase would produce cyclic AMP, which in turn would gate membrane channels and increase the ciliary conductance. All but seven of the cilia showed some conductance increase in the presence of ATP. This conductance was increased by GTPγS, which stimulates the cyclase (Pace *et al.* 1985; Sklar *et al.* 1986; Shirley *et al.* 1986; Bruch and Teeter, 1990; Boekhoff *et al.* 1990). However, the ratio of unstimulated to GTPγS-stimulated conductances varied widely across the population of cilia (Fig. 6A,B). Some cilia

showed almost no conductance in the absence of GTPγS but a large conductance in its presence. In these cilia, G-protein-mediated activation of the cyclase by odorants would be expected to generate a signal much larger than the baseline noise. Other cilia, however, showed large ATP-dependent conductances even in the absence of GTPγS. The resulting large inward current could continually depolarize the cell unless a compensating level of phosphodiesterase activity were present. Nonetheless, substantial unstimulated cyclase activity has been observed in suspensions enriched in olfactory cilia as well (Pace *et al.* 1985; Sklar *et al.* 1986; Shirley *et al.* 1986; Bruch and Teeter, 1990; Boekhoff *et al.* 1990).

We do not know why the conductance activated by ATP alone varies so widely from one cilium to the next. Perhaps two types of cyclase are present, one constitutively active and the other activated only by G-proteins. Alternatively, it is conceivable that the cyclase can be covalently modified and thus exist in more than one state. Our evidence is consistent with a conductance that depends on cyclase activity. However, it remains to be seen whether ATP and GTPγS influence ciliary conductance by other mechanisms.

We have found that conductance properties vary widely across the population of olfactory cilia. Cells bearing cilia of high basal conductance may have lower input resistances and be less sensitive to weak stimuli. The presence of cilia with constitutively active adenylate cyclase could depolarize the cell, resulting in a high basal firing rate. Cells with little ciliary cyclic-AMP-activated current available might generate undetectably small odorant responses. We have not yet studied the odorant specificities of individual cilia. However, it seems likely that olfactory cilia will also be found to be highly variable in their expression of odorant receptor molecules (Buck, 1992).

Appendix: the olfactory cilium as a one-dimensional cable

Outline of problems and assumptions

The technique of pulling a single cilium into a patch pipette and forming a tight seal at its base allows one to measure the input impedance of what amounts to an open-circuited short cable. If the response of this cable to the middle portion of a very slow voltage ramp is determined, then we have an estimate of the input resistance of the cable. This is true given that the voltages applied are in the linear response range of the ciliary membrane conductances. From known properties of linear finite cables and the assumptions of uniform distribution of conductance over the ciliary surface and uniform conductivity of the core, it is possible to estimate the surface conductance of the cilium. Since almost all of the surface conductance is due to relatively voltage-insensitive channels, we can estimate channel density from the surface conductance per unit area, the single-channel conductance and the channel's open probability. The open end of the cilium is assumed to be at bath potential, and the membrane in contact with the pipette solution is at the voltage-clamp potential. The voltage drop with distance is assumed to occur along the internal core of the cilium, and the internal membrane surface is at the same potential as the core.

Application of finite cable theory

The input resistance of a finite cable of length l is given by equation 4.11 of Jack *et al.* (1983):

$$\frac{V_0}{I} = r_a \lambda \coth\left(\frac{l}{\lambda}\right), \tag{1}$$

where V_0 is the voltage at the open end of the fiber, I is the current entering the open end, r_a is the intracellular resistance per unit length of cable, λ is the space constant and l is the length of the cable. Note that for the special case $l \gg \lambda$, the hyperbolic cotangent term approaches unity and the relationship then predicts the input resistance of a semi-infinite cable. However, the full equation 1 was used as shown in all analyses. The input resistance V_0/I will be defined here as R_{in}. Neglecting the resistance of the extraciliary fluid r_o (due to the large volume in the patch electrode surrounding the cilium) allows us to define λ [after equation 3.10 of Jack *et al.* (1983)]:

$$\lambda = \sqrt{\frac{r_m}{r_a}}, \tag{2}$$

where r_m is the membrane resistance per unit of length. In addition, we can relate the constants r_m and r_a for a unit length of cable to R_m, the resistance of a unit area of membrane, R_i, the resistivity of the lumen, and D, the diameter, by the following (after Jack *et al.* 1983, p. 27):

$$r_m = \frac{R_m}{\pi D} \tag{3}$$

and

$$r_a = \frac{4R_i}{\pi D^2}. \tag{4}$$

Substituting equations 3 and 4 into equation 2 yields:

$$\lambda = \sqrt{\frac{DR_m}{4R_i}}. \tag{5}$$

Substituting equations 4 and 5 into equation 1 then gives:

$$R_{in} = \sqrt{\frac{4R_i R_m}{\pi^2 D^3}} \coth\left(\frac{l}{\lambda}\right). \tag{6}$$

Squaring both sides and dividing through by R_m and R_{in}^2 yields:

$$\frac{1}{R_m} = \frac{4R_i}{\pi^2 D^3 R_{in}^2}\left[\coth\left(\frac{l}{\lambda}\right)\right]^2. \tag{7}$$

Defining the specific membrane conductance, $G_m = 1/R_m$, and the input conductance, $G_{in} = 1/R_{in}$, and substituting into equation 7 gives:

$$G_m = \frac{4R_i G_{in}^2}{\pi^2 D^3}\left[\coth\left(\frac{l}{\lambda}\right)\right]^2. \quad (8)$$

Substituting G_m for $1/R_m$ in the definition of λ given in equation 5 yields:

$$\lambda = \sqrt{\frac{D}{4R_i G_m}}. \quad (9)$$

The resistivity of the pseudointracellular solution R_i was estimated to be $70\,\Omega$ cm. The proximal portion of a frog olfactory cilium has a diameter (D) of 0. 28 μm (Menco, 1980). It was necessary to solve for the unknowns λ and G_m. G_m can be eliminated from equations 8 and 9 to give:

$$\coth\left(\frac{l}{\lambda}\right) = \frac{\pi D^2}{4R_i G_{in}}\frac{1}{\lambda}. \quad (10)$$

Equation 10 is a transcendental equation in λ, and the FindRoot function of Mathematica software (Wolfram Research, Inc., Champaign, IL) was able to find roots for λ given a starting value of 3 μm using the Newton–Raphson method. Substituting this value of λ into equation 8 permitted calculation of G_m, the specific membrane conductance reported throughout the Results section.

The primary source of error in these calculations comes from the assumed ciliary diameter D; note in equation 8 that G_m has an inverse third-order dependence on D. In the more conductive cilia, most of the measured current arose from the proximal part of the cilium, so we assumed the proximal diameter (0.28 μm). In fact, the distal cilium tapers to a diameter of 0.19 μm (Menco, 1980). Assuming a ciliary diameter that is an average of the proximal and distal diameters (D=0.24 μm) reduces the calculated space constant λ. For a cilium many times longer than λ, the reduction is 27 %. For the least conductive cilia ($l \ll \lambda$), the reduction of λ is just 14 %. At the same time, assuming the smaller diameter increases the estimated specific conductance G_m. For a cilium many times longer than λ, the increase is 59 %. For the least conductive cilia, the increase in G_m is 17 %. Assuming the smaller diameter of 0.24 μm did not change the significance of the correlations presented in the Results.

We have previously presented several dose–response studies based directly on measured input conductance. Such results accurately describe effects on current measured at the base of the cilium. However, to estimate effects on a local patch of membrane, the results must be corrected for the ciliary cable properties. The ciliary Cl^- current, for example, was found to be half-activated by 4.8 μmol l^{-1} Ca^{2+} with a Hill coefficient of 2.0 (Kleene and Gesteland, 1991*b*). Correction of the raw data to give specific conductances increases the half-maximal $[Ca^{2+}]_{free}$ to 6.0 μmol l^{-1}. The Hill coefficient is unchanged. In inhibition studies, IC_{50} values are decreased somewhat by the cable correction. We reported, for example, that niflumic acid inhibits the Cl^- input conductance with an IC_{50} of 44 μmol l^{-1} (Kleene, 1993*b*). After correction for the ciliary cable properties, this value decreases to 22 μmol l^{-1}. Ciliary lengths were not measured

in the dose–response studies, so for correction we assumed a length of 32 μm. This was the average of 209 cilia not selected on the basis of length (Kleene and Gesteland, 1991*a*).

We are grateful to Chunsong Luo and John Teeter for helpful discussion, to Gregory Kaczorowski for a gift of DCB, to Barbara Cincush for expert technical assistance and to Scott Michaels and David Smith for statistical consulting. This work was supported by National Institutes of Health grants R55 DC00926, R01 DC00926, P01 DC00347 and RO1 DC00352.

References

ADAMEK, G. D., GESTELAND, R. C., MAIR, R. G. AND OAKLEY, B. (1984). Transduction physiology of olfactory receptor cilia. *Brain Res.* **310**, 87–97.

BERS, D. M. (1982). A simple method for the accurate determination of free [Ca] in Ca-EGTA solutions. *Am. J. Physiol.* **242**, C404–C408.

BOEKHOFF, I., TAREILUS, E., STROTMANN, J. AND BREER, H. (1990). Rapid activation of alternative second messenger pathways in olfactory cilia from rats by different odorants. *EMBO J.* **9**, 2453–2458.

BRUCH, R. C. AND TEETER, J. H. (1990). Cyclic AMP links amino acid chemoreceptors to ion channels in olfactory cilia. *Chem. Senses* **15**, 419–430.

BUCK, L. B. (1992). The olfactory multigene family. *Current Opinion Neurobiol*. **2**, 282–288.

CHEN, T.-Y. AND YAU, K.-W. (1994). Direct modulatation by Ca^{2+}-calmodulin of cyclic nucleotide-activated channel of rat olfactory receptor neurons. *Nature* **368**, 545–548.

DHALLAN, R. S., YAU, K.-W., SCHRADER, K. A. AND REED, R. R. (1990). Primary structure and functional expression of a cyclic nucleotide-activated channel from olfactory neurons. *Nature* **347**, 184–187.

DIONNE, V. (1992). Chemosensory responses in isolated olfactory receptor neurons from *Necturus maculosus*. *J. gen. Physiol.* **99**, 415–433.

DUBIN, A. E. AND DIONNE, V. E. (1994). Action potentials and chemosensitive conductances in the dendrites of olfactory neurons suggest new features for odor transduction. *J. gen. Physiol.* **103**, 181–201.

FADOOL, D. A. AND ACHE, B. W. (1992). Plasma membrane inositol 1,4,5-trisphosphate-activated channels mediate signal transduction in lobster olfactory receptor neurons. *Neuron* **9**, 907–918.

FIRESTEIN, S., DARROW, B. AND SHEPHERD, G. M. (1991). Activation of the sensory current in salamander olfactory receptor neurons depends on a G protein-mediated cyclic AMP messenger system. *Neuron* **6**, 825–835.

FIRESTEIN, S., SHEPHERD, G. M. AND WERBLIN, F. (1990). Time course of the membrane current underlying sensory transduction in salamander olfactory receptor neurones. *J. Physiol., Lond.* **430**, 135–158.

FRINGS, S. AND LINDEMANN, B. (1991). Current recording from sensory cilia of olfactory receptor cells *in situ*. I. The neuronal response to cyclic nucleotides. *J. gen. Physiol.* **97**, 1–16.

FRINGS, S., LYNCH, J. W. AND LINDEMANN, B. (1992). Properties of cyclic nucleotide-gated channels mediating olfactory transduction. *J. gen. Physiol.* **100**, 45–67.

GARCIA, M. L., KING, V. F., SHEVELL, J. L., SLAUGHTER, R. S., SUAREZ-KURTZ, G., WINQUIST, R. J. AND KACZOROWSKI, G. J. (1990). Amiloride analogs inhibit L-type calcium channels and display calcium entry blocker activity. *J. biol. Chem.* **265**, 3763–3771.

GETCHELL, T. V. (1986). Functional properties of vertebrate olfactory receptor neurons. *Physiol. Rev.* **66**, 772–818.

HAGIWARA, S. AND OHMORI, H. (1982). Studies of calcium channels in rat clonal pituitary cells with patch electrode voltage clamp. *J. Physiol., Lond.* **331**, 231–252.

HUQUE, T. AND BRUCH, R. C. (1986). Odorant- and guanine nucleotide-stimulated phosphoinositide turnover in olfactory cilia. *Biochem. biophys. Res. Commun.* **137**, 36–42.

JACK, J. J. B., NOBLE, D. AND TSIEN, R. W. (1983). *Electric Current Flow in Excitable Cells*. Oxford: Clarendon Press.

KARPEN, J. W., LONEY, D. A. AND BAYLOR, D. A. (1992). Cyclic GMP-activated channels of salamander retinal rods: spatial distribution and variation of responsiveness. *J. Physiol., Lond.* **448**, 257–274.

KLEENE, S. J. (1992). Basal conductance of frog olfactory cilia. *Pflügers Arch.* **421**, 374–380.
KLEENE, S. J. (1993*a*). The cyclic nucleotide-activated conductance in olfactory cilia: effects of cytoplasmic Mg^{2+} and Ca^{2+}. *J. Membr. Biol.* **131**, 237–243.
KLEENE, S. J. (1993*b*). Origin of the chloride current in olfactory transduction. *Neuron* **11**, 123–132.
KLEENE, S. J. AND GESTELAND, R. C. (1991*a*). Transmembrane currents in frog olfactory cilia. *J. Membr. Biol.* **120**, 75–81.
KLEENE, S. J. AND GESTELAND, R. C. (1991*b*). Calcium-activated chloride conductance in frog olfactory cilia. *J. Neurosci.* **11**, 3624–3629.
KOLESNIKOV, S. S., ZHAINAZAROV, A. B. AND KOSOLAPOV, A. V. (1990). Cyclic nucleotide-activated channels in the frog olfactory receptor plasma membrane. *FEBS Lett.* **266**, 96–98.
KURAHASHI, T. (1989). Activation by odorants of cation-selective conductance in the olfactory receptor cell isolated from the newt. *J. Physiol., Lond.* **419**, 177–192.
KURAHASHI, T. (1990). The response induced by intracellular cyclic AMP in isolated olfactory receptor cells of the newt. *J. Physiol., Lond.* **430**, 355–371.
KURAHASHI, T. AND KANEKO, A. (1993). Gating properties of the cyclic AMP-gated channel in toad olfactory receptor cells. *J. Physiol., Lond.* **466**, 287–302.
KURAHASHI, T. AND YAU, K.-W. (1993). Co-existence of cationic and chloride components in odorant-induced current of vertebrate olfactory receptor cells. *Nature* **363**, 71–74.
LIDOW, M. S., GESTELAND, R. C., SHIPLEY, M. T. AND KLEENE, S. J. (1987). Comparative study of immature and mature olfactory receptor cells in adult frogs. *Dev. Brain Res.* **31**, 243–258.
LOWE, G. AND GOLD, G. H. (1991). The spatial distributions of odorant sensitivity and odorant-induced currents in salamander olfactory receptor cells. *J. Physiol., Lond.* **442**, 147–168.
LOWE, G. AND GOLD, G. H. (1993*a*). Contribution of the ciliary cyclic nucleotide-gated conductance to olfactory transduction in the salamander. *J. Physiol., Lond.* **462**, 175–196.
LOWE, G. AND GOLD, G. H. (1993*b*). Nonlinear amplification by calcium-dependent chloride channels in olfactory receptor cells. *Nature* **366**, 283–286.
MAIR, R. G., GESTELAND, R. C. AND BLANK, D. L. (1982). Changes in morphology and physiology of olfactory receptor cilia during development. *Neuroscience* **7**, 3091–3103.
MENCO, B. PH. M. (1980). Qualitative and quantitative freeze-fracture studies on olfactory and nasal respiratory structures in frog, ox, rat and dog. I. A general survey. *Cell Tissue Res.* **207**, 183–209.
MENCO, B. PH. M., TEKULA, F. D., FARBMAN, A. I. AND DANHO, W. (1994). G-proteins and type III adenylyl cyclase during rat olfactory epithelium ontogeny. In *Olfaction and Taste*, vol. XI (ed. K. Kurihara, N. Suzuki and H. Ogawa), pp. 141–144. Berlin: Springer-Verlag.
MIYAMOTO, T., RESTREPO, D., CRAGOE, E. J. AND TEETER, J. H. (1992). IP_3- and cAMP-induced responses in isolated olfactory receptor neurons from the channel catfish. *J. Membr. Biol.* **127**, 173–183.
NAKAMURA, T. AND GOLD, G. H. (1987). A cyclic nucleotide-gated conductance in olfactory receptor cilia. *Nature* **325**, 442–444.
NAKAMURA, T. AND GOLD, G. H. (1988). Single channel properties of the ciliary cyclic nucleotide-gated conductance. *Chem. Senses* **13**, 723–724.
OKADA, Y., TEETER, J. H. AND RESTREPO, D. (1994). Inositol 1,4,5-trisphosphate-gated conductance in isolated rat olfactory neurons. *J. Neurophysiol.* **71**, 595–602.
PACE, U., HANSKI, E., SALOMON, Y. AND LANCET, D. (1985). Odorant-sensitive adenylate cyclase may mediate olfactory reception. *Nature* **316**, 255–258.
PUN, R. Y. K. AND GESTELAND, R. C. (1991). Somatic sodium channels of frog olfactory receptor neurones are inactivated at rest. *Pflügers Arch.* **418**, 504–511.
RESTREPO, D., BOEKHOFF, I. AND BREER, H. (1993). Rapid kinetic measurements of second messenger formation in olfactory cilia from channel catfish. *Am. J. Physiol.* **264**, C906–C911.
RESTREPO, D., MIYAMOTO, T., BRYANT, B. P. AND TEETER, J. H. (1990). Odor stimuli trigger influx of calcium into olfactory neurons of the channel catfish. *Science* **249**, 1166–1168.
RESTREPO, D., TEETER, J. H., HONDA, E., BOYLE, A. G., MARECEK, J. F., PRESTWICH, G. D. AND KALINOSKI, D. L. (1992). Evidence for an $InsP_3$-gated channel protein in isolated rat olfactory cilia. *Am. J. Physiol.* **263**, C667–C673.
SHIRLEY, S. G., ROBINSON, C. J., DICKINSON, K., AUJLA, R. AND DODD, G. H. (1986). Olfactory adenylate cyclase of the rat. *Biochem. J.* **240**, 605–607.
SKLAR, P. B., ANHOLT, R. R. H. AND SNYDER, S. H. (1986). The odorant-sensitive adenylate cyclase of olfactory receptor cells. *J. biol. Chem.* **261**, 15538–15543.

SUZUKI, N. (1993). The role of IP_3-activated ion channels in frog olfactory transduction. *Chem. Senses* **18**, 339.

TSIEN, R. (1980). New calcium indicators and buffers with high selectivity against magnesium and protons: design, synthesis and properties of prototype structures. *Biochemistry, N.Y.* **19**, 2396–2404.

ZUFALL, F. AND FIRESTEIN, S. (1993). Divalent cations block the cyclic nucleotide-gated channel of olfactory receptor neurons. *J. Neurophysiol.* **69**, 1758–1768.